

# In vitro and in vivo evaluation of [<sup>18</sup>F]ciprofloxacin for the imaging of bacterial infections with PET

Oliver Langer<sup>1</sup>, Martin Brunner<sup>1</sup>, Markus Zeitlinger<sup>1</sup>, Sophie Ziegler<sup>2</sup>, Ulrich Müller<sup>1</sup>, Georg Dobrozemsky<sup>3, 4</sup>, Edith Lackner<sup>1</sup>, Christian Joukhadar<sup>1</sup>, Markus Mitterhauser<sup>3</sup>, Wolfgang Wadsak<sup>3</sup>, Erich Minar<sup>2</sup>, Robert Dudczak<sup>3</sup>, Kurt Kletter<sup>3</sup>, Markus Müller<sup>1</sup>

<sup>1</sup> Division of Clinical Pharmacokinetics, Department of Clinical Pharmacology, Medical University Vienna, Vienna, Austria

<sup>2</sup> Division of Angiology, Department of Internal Medicine II, Medical University Vienna, Vienna, Austria

<sup>3</sup> Department of Nuclear Medicine, Medical University Vienna, Vienna, Austria

<sup>4</sup> Department of Biomedical Engineering and Physics, Medical University Vienna, Vienna, Austria

Received: 2 June 2004 / Accepted: 29 June 2004 / Published online: 4 September 2004

© Springer-Verlag 2004

**Abstract.** *Purpose:* The suitability of the <sup>18</sup>F-labelled fluoroquinolone antibiotic ciprofloxacin ([<sup>18</sup>F]ciprofloxacin) for imaging of bacterial infections with positron emission tomography (PET) was assessed in vitro and in vivo. *Methods:* For the in vitro experiments, suspensions of various *E. coli* strains were incubated with different concentrations of [<sup>18</sup>F]ciprofloxacin (0.01–5.0 µg/ml) and radioactivity retention was measured in a gamma counter. For the in vivo experiments, 725 ± 9 MBq [<sup>18</sup>F]ciprofloxacin was injected intravenously into four patients with microbiologically proven bacterial soft tissue infections of the lower extremities and time-radioactivity curves were recorded in infected and uninfected tissue for 5 h after tracer injection. *Results:* Binding of [<sup>18</sup>F]ciprofloxacin to bacterial cells was rapid, non-saturable and readily reversible. Moreover, bacterial binding of the agent was similar in ciprofloxacin-resistant and ciprofloxacin-susceptible clinical isolates. These findings suggest that non-specific binding rather than specific binding to bacterial type II topoisomerase enzymes is the predominant mechanism of bacterial retention of the radiotracer. PET studies in the four patients with microbiologically proven bacterial soft tissue infections demonstrated locally increased radioactivity uptake in infected tissue, with peak ratios between infected and uninfected tissue ranging from 1.8 to 5.5. Radioactivity was not retained in infected tissue and appeared to wash out with a similar elimination half-life as in uninfected tissue, suggesting that the kinetics of [<sup>18</sup>F]ciprofloxacin in infected tissue are governed by increased blood flow

and vascular permeability due to local infection rather than by a binding process. *Conclusion:* Taken together, our results indicate that [<sup>18</sup>F]ciprofloxacin is not suited as a bacteria-specific infection imaging agent for PET.

**Keywords:** Ciprofloxacin – Fluorine-18 – Positron emission tomography – Infection imaging – Human

**Eur J Nucl Med Mol Imaging (2005) 32:143–150**

DOI 10.1007/s00259-004-1646-2

## Introduction

In order to improve the clinical management of patients with fever of unknown origin or prosthetic joint infection, the availability of a single-photon emission computed tomography (SPECT) or positron emission tomography (PET) imaging agent that is able to differentiate between infection caused by bacteria and sterile inflammation would be desirable [1]. One approach to the development of such a tracer is the use of radiolabelled antibiotic agents that bind in vivo specifically to bacterial cells. This approach has been exemplified by a complex of <sup>99m</sup>Tc with the fluoroquinolone antibiotic ciprofloxacin [2, 3] as well as by <sup>99m</sup>Tc-labelled antimicrobial peptides, such as <sup>99m</sup>Tc-UBI 29–41 [4, 5]. Although the exact chemical structure of <sup>99m</sup>Tc-ciprofloxacin, also known as Infecton (Draximage, Inc.), has not yet been determined, the radiolabelled compound is believed to retain the pharmacokinetic and pharmacodynamic properties of unlabelled ciprofloxacin and to accumulate in vivo within bacterial cells [6].

Fluoroquinolone antibiotics exert their antimicrobial effect by inhibition of the bacterial type II topoisomerase enzymes DNA gyrase and/or topoisomerase IV. This action is mediated by fluoroquinolone binding to enzyme

Oliver Langer (✉)  
Division of Clinical Pharmacokinetics,  
Department of Clinical Pharmacology,  
Medical University Vienna,  
Währinger Gürtel 18–20, 1090 Vienna, Austria  
e-mail: oliver.langer@meduniwien.ac.at  
Tel.: +43-1-404002981, Fax: +43-1-404002998

and bacterial DNA in the form of a ternary complex [7]. Some fluoroquinolones, such as ciprofloxacin, show relatively little metabolism in vivo, with the majority of drug (>85%) being excreted in unchanged form [8]. Since ciprofloxacin is a registered antibiotic for human use, no safety concerns are expected to arise from its use for clinical imaging. These characteristics, along with the presence of fluorine in its native structure, make ciprofloxacin a promising candidate for the development of a bacteria-specific infection imaging agent for PET.

We have recently labelled ciprofloxacin with  $^{18}\text{F}$  (half-life 109.8 min) [9, 10] and have assessed the pharmacokinetics of [ $^{18}\text{F}$ ]ciprofloxacin in healthy volunteers [11]. We reasoned that [ $^{18}\text{F}$ ]ciprofloxacin might be an alternative to  $^{99\text{m}}\text{Tc}$ -ciprofloxacin for infection imaging, exploiting the advantages of the PET technique, i.e. better spatial resolution, increased sensitivity and quantitative data on radioactivity distribution. In the present work, first PET data in patients with microbiologically proven bacterial infections are reported. Moreover, in vitro bacterial binding experiments were performed in order to elucidate the mechanism of binding of the radio-tracer to bacterial cells.

## Materials and methods

### Synthesis and quality control of [ $^{18}\text{F}$ ]ciprofloxacin

[ $^{18}\text{F}$ ]Ciprofloxacin was prepared by a two-step radiosynthesis as previously described [9, 10]. The purified radiotracer was formulated in 7 ml sterile phosphate buffer (0.2 M, pH 5.5–6.0). For intravenous administration, an aliquot of the product solution was diluted with physiological saline solution to an injection volume of 10 ml. Prior to injection into patients, quality control was performed for each batch of synthesised [ $^{18}\text{F}$ ]ciprofloxacin as previously described [9]. As assessed by analytical high-performance liquid chromatography (HPLC) and thin-layer chromatography (TLC), the radiochemical purity of [ $^{18}\text{F}$ ]ciprofloxacin was >99% and the chemical purity exceeded 95%. The specific radioactivity of [ $^{18}\text{F}$ ]ciprofloxacin was determined by analytical reversed-phase HPLC using a calibration curve generated from known amounts of unlabelled ciprofloxacin [9]. The mean specific radioactivity of [ $^{18}\text{F}$ ]ciprofloxacin at the time of injection was  $342 \pm 94$  MBq/ $\mu\text{mol}$  ( $n=4$ ). Therefore, an injected amount of 725 MBq [ $^{18}\text{F}$ ]ciprofloxacin corresponded to approximately 2.1  $\mu\text{mol}$  or 0.8 mg of unlabelled ciprofloxacin. For in vitro bacteria binding experiments the formulated [ $^{18}\text{F}$ ]ciprofloxacin solution was diluted with phosphate buffer (100 mM, pH 7.0) to obtain a final ciprofloxacin concentration of 1.0  $\mu\text{g}/\text{ml}$ .

### Bacterial strains and growth conditions

*Escherichia coli* (ATCC 25922) was obtained from LGC Promochem (Wesel, Germany). Clinical isolates of *E. coli* with different susceptibility to ciprofloxacin [minimum inhibitory concentration (MIC)=0.015, 0.25, 8 and 16  $\mu\text{g}/\text{ml}$ ] were obtained from the Department of Infectious Diseases and Chemotherapy, General Hospital Vienna, Austria. All bacteria were stored in liquid nitrogen ( $-196^\circ\text{C}$ ) prior to use. Bacteria were first grown overnight on

Columbia agar plates (Columbia + 5% sheep blood, BioMerieux, France) at  $37^\circ\text{C}$ . Afterwards bacteria were grown overnight in Mueller-Hinton broth (Merck, Darmstadt, Germany) at  $37^\circ\text{C}$ . Bacterial inoculum was estimated using either the microdilution method or a turbidity meter (A-just, Abbott, North Chicago, USA). Bacterial suspensions were centrifuged (15 min, 2,500g, room temperature) with a Rotanta/TRC centrifuge (Hettich, Tuttlingen, Germany). The obtained pellet containing the bacterial cells was then re-suspended in a calculated volume of aqueous phosphate buffer (100 mM, pH 7.0) according to the desired bacterial inoculum (colony forming units/ml, CFU/ml). Bacterial concentrations ranged from  $1 \times 10^8$  CFU/ml to  $1 \times 10^9$  CFU/ml. The suspension was afterwards aliquoted in 3-ml portions into 12-ml Sorvall polyallomer tubes (Du Pont Company, Wilmington, DE, USA). For some experiments the MIC values of the used bacterial strains were determined by a twofold serial Mueller-Hinton microdilution method, according to National Committee for Clinical Laboratory Standards (NCCLS) criteria [12]. In this method, bacteria were pre-cultured overnight on Columbia agar plates and then introduced at an initial inoculum of approximately  $5 \times 10^5$  CFU/ml into Mueller-Hinton broth containing ciprofloxacin. The lowest concentration of antibiotic, which inhibited visible bacterial growth after 20 h of incubation at  $37^\circ\text{C}$ , was defined as the MIC.

### Determination of bacterial binding of [ $^{18}\text{F}$ ]ciprofloxacin

The experimental conditions employed for this study were adapted from previous work [13]. Bacterial suspensions were allowed to equilibrate for 10 min at  $37^\circ\text{C}$  in a gently shaking water bath. At the end of the equilibration period, appropriate amounts of [ $^{18}\text{F}$ ]ciprofloxacin (i.e. 50–200 kBq) in phosphate buffer were added. For the binding curve shown in Fig. 1, bacteria were incubated with a range of ciprofloxacin concentrations (0.01–5.0  $\mu\text{g}/\text{ml}$ ) by addition of unlabelled ciprofloxacin to the radioligand. Afterwards, the tubes containing bacteria and radiolabelled ciprofloxacin were incubated for 10–20 min at  $37^\circ\text{C}$  in the water bath. Then, the bacterial suspensions were centrifuged (5 min, 12,000g,  $4^\circ\text{C}$ ) in a Sorvall RC-5C refrigerated centrifuge. The supernatants were discarded and the cell pellets were washed with 8 ml ice-cooled phosphate buffer to remove unbound radioactivity. After centrifugation (5 min, 12,000g,  $4^\circ\text{C}$ ) and removal of supernatant, the pellets were re-suspended in fresh phosphate buffer (2 ml) and transferred into new tubes. The cell suspensions were measured in a Packard Cobra II auto-gamma counter (Packard Instrument Company, Meriden, USA). In order to correct for non-specific binding, blank tubes containing only phosphate buffer were also incubated with [ $^{18}\text{F}$ ]ciprofloxacin. In some experiments, unlabelled norfloxacin (100  $\mu\text{g}/\text{ml}$ ) was added at the beginning of the equilibration period to the incubation buffer. Samples were then incubated with [ $^{18}\text{F}$ ]ciprofloxacin and further processed as described above. In other experiments, the efflux of [ $^{18}\text{F}$ ]ciprofloxacin from bacterial cell pellets was assessed. In these experiments [ $^{18}\text{F}$ ]ciprofloxacin-loaded cell pellets were re-incubated with 3 ml phosphate buffer at  $37^\circ\text{C}$  and then processed as described earlier. The measured radioactivity values were related to the mass of ciprofloxacin via the decay-corrected specific radioactivity of [ $^{18}\text{F}$ ]ciprofloxacin. Bacterial uptake of ciprofloxacin was expressed as nanogram retained mciprofloxacin per  $\mu\text{g}/\text{ml}$  ciprofloxacin in the incubation medium per  $1 \times 10^9$  CFU/ml bacterial cells [ $\text{ng}/(\mu\text{g}/\text{ml}) \times (10^9 \text{ CFU}/\text{ml})$ ]. All experiments were performed in triplicate and results were expressed as the mean  $\pm$  standard deviation.

## PET study in patients

The study was approved by the local Ethics Committee. All patients were given a detailed description of the study and their written consent was obtained. The study was performed in accordance with the Declaration of Helsinki and the Good Clinical Practice Guideline of the European Commission (EC-GCP guideline). Four patients [three males, one female; mean weight  $78 \pm 24$  (standard deviation, SD) kg; mean height  $173 \pm 18$  cm; mean age  $76 \pm 14$  years] with microbiologically proven bacterial soft tissue infections of the lower extremities were included in the study. Three patients presented with peripheral arterial occlusive disease and one with chronic venous insufficiency (patient 1). Each patient was subjected to a screening examination including medical history, physical examination, 12-lead ECG, complete blood count, serum electrolytes, creatinine, BUN, total bilirubin, gamma-GT, AST, ALT, total protein, aPTT, normotest, and HBs antigen, HCV antibody and HIV antibody tests. Prior to inclusion in the study and on the day of the PET study, swabs were taken from the centre of the wound and microbiological specimens were cultured on appropriate media. Isolates were identified by conventional means in the local microbiological laboratory (see Table 2). Bacterial isolates were tested for susceptibility to ciprofloxacin. Patients were excluded if they received therapy with a quinolone antibiotic within 1 week before the start of the study.

On the day of the study, a venous catheter was placed in each arm (one for infusion of radiolabelled drug, one for blood sampling). Patients were positioned supine on the scanner bed with the infected and uninfected limbs within the field of view (FOV) of the PET camera. PET images were acquired with a GE Advance PET scanner (GE Medical Systems, Wukessa, WI) with a transverse FOV of 55 cm and an axial FOV of 15 cm. In order to correct for tissue attenuation of photons, a transmission scan of 10 min duration using two 400-MBq  $^{68}\text{Ge}$  pin sources was recorded prior to radiotracer injection. Then [ $^{18}\text{F}$ ]ciprofloxacin (mean injected amount  $725 \pm 9$  MBq) was administered as an intravenous bolus. Serial PET imaging and venous blood sampling were initiated at the start of bolus infusion and were continued for 5 h. The imaging protocol consisted of the following frame sequence: during the first 60 min after injection, dynamic images of the infected and uninfected limb were acquired (frame lengths  $12 \times 5$  min). Subjects were then allowed to resume usual activity. Approximately 2, 3, 4 and 5 h after tracer injection, subjects were re-positioned in the PET camera. At each time point a transmission scan (3-min duration) followed by an emission scan over three axial FOVs with a scan duration of 5 min per FOV was performed. During the study period, venous blood samples (9 ml) were collected at 1, 3, 5, 15, 30, 45, 60, 90, 120, 150, 180, 240 and 300 min following radiotracer injection. Plasma was obtained by centrifugation at 3,000 rpm for 10 min. Aliquots of whole blood and plasma (1 ml each) were measured in a Packard Cobra II auto-gamma counter that had been cross-calibrated with the PET camera. Radioactivity counting rates were decay corrected to the time of tracer injection and normalised to the injected radiotracer amount in order to generate plasma and whole blood time-radioactivity curves (TACs).

### Binding of [ $^{18}\text{F}$ ]ciprofloxacin to blood cells

In order to study the reversibility of [ $^{18}\text{F}$ ]ciprofloxacin binding to blood cells, blood samples were obtained from one patient after injection of [ $^{18}\text{F}$ ]ciprofloxacin. The samples were centrifuged at 3,500 rpm for 10 min, the supernatant was removed and the pellets

containing cellular components of blood were counted in a gamma counter. Subsequently, cell pellets were re-suspended in either 1.0 ml plasma (obtained from the same patient before radiotracer injection) or 1.0 ml phosphate buffer (100 mM, pH 7.0) and incubated for 10 min at 37°C. After incubation, samples were centrifuged and cell pellet and supernatant were separately counted in a gamma counter in order to determine the distribution of radioactivity.

### PET data analysis

Reconstruction of the PET data was performed by means of iterative reconstruction using the ordered subsets–expectation maximisation method with 28 subsets and two iterations. The loop filter (Gaussian) was set to a full-width at half-maximum (FWHM) of 4.3 mm, and a post-filtering algorithm of 6.00 mm FWHM was applied. Attenuation correction was performed using the manufacturer's segmentation algorithm for transmission data. Equally sized regions of interest were drawn in the reconstructed summation image over the infected area and the contralateral uninfected side and transferred to all other images of the time sequence. Radioactivity concentrations (in kBq/ml), corrected for radioactive decay to the time of tracer injection, were calculated. Since the density of the studied tissue was approximately 1 g/ml, concentrations expressed as kBq/ml were considered equal to concentrations expressed as kBq/g tissue. Radioactivity concentrations were normalised to the injected radiotracer amount and expressed as standardised uptake values (SUVs). The SUV is dimensionless and defined as the local radioactivity concentration (in kBq/g) divided by the administered radioactivity amount per gram body weight (kBq/g). The radioactivity concentration data were combined to provide TACs for the whole observation period. The TACs were used to calculate the following pharmacokinetic parameters using the Kinetic 2000 version 3.0 (InnaPhase Corporation, Philadelphia, USA) software package: peak concentration ( $C_{\text{max}}$ , SUV  $\pm$  SD), time to reach peak concentration ( $T_{\text{max}}$ , minutes  $\pm$  SD) and terminal elimination half-life ( $T_{1/2}$ , minutes  $\pm$  SD). Data within individuals were statistically compared using the Wilcoxon matched pairs test.

## Results

### *In vitro* bacterial binding of [ $^{18}\text{F}$ ]ciprofloxacin

The binding of [ $^{18}\text{F}$ ]ciprofloxacin to *E. coli* ATCC 25922 was linear over a concentration range of 0.01–5.0  $\mu\text{g/ml}$  ( $R=0.99603$ ;  $P<0.0001$ ) [(Fig. 1)]. The average binding of [ $^{18}\text{F}$ ]ciprofloxacin to *E. coli* was  $55 \pm 2$  ng/( $\mu\text{g/ml}$ )  $\times$  ( $10^9$  CFU/ml) ( $n=9$ ). Binding to bacteria was rapid, with binding equilibrium achieved within the first 5 min after tracer incubation. Prolongation of the incubation time to 120 min exerted no effect on the bacterial binding of [ $^{18}\text{F}$ ]ciprofloxacin. For practical reasons an incubation time of 10–20 min was chosen for all the following experiments.

In order to study the mechanism of [ $^{18}\text{F}$ ]ciprofloxacin binding to bacteria, an excess of the unlabelled fluoroquinolone norfloxacin was added to the incubation buffer prior to addition of the radiotracer. [ $^{18}\text{F}$ ]Ciprofloxacin binding was descriptively similar in norfloxacin pre-

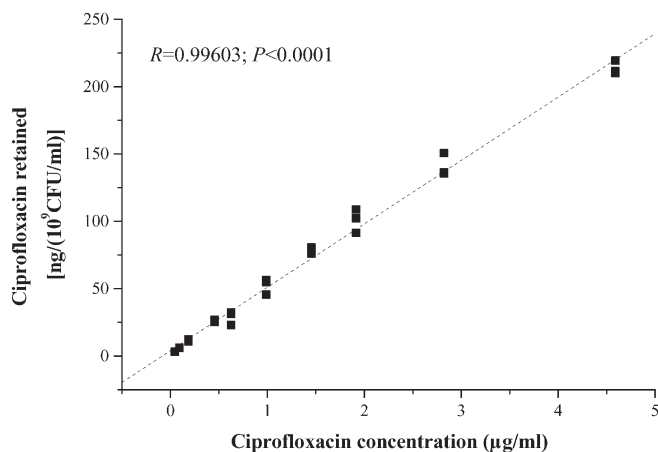


**Fig. 1.** In vitro binding of [ $^{18}\text{F}$ ]ciprofloxacin to *E. coli* ATCC 25922 employing different concentrations of ciprofloxacin (in  $\mu\text{g/ml}$ ) in the incubation buffer. The coefficient of correlation ( $R$ ) and the corresponding  $P$  value obtained from linear regression analysis are displayed

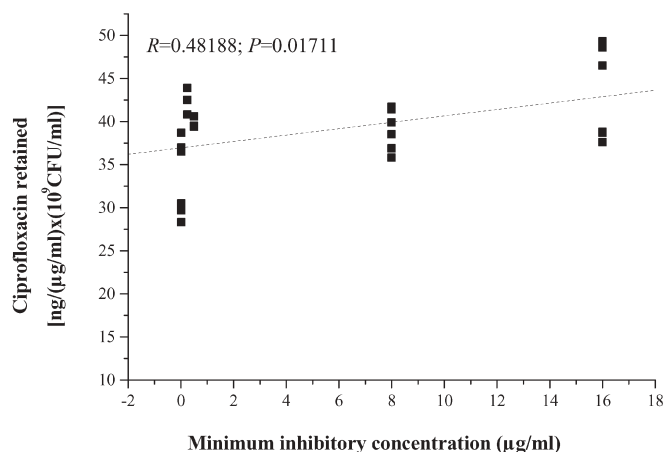


**Fig. 2.** In vitro binding of [ $^{18}\text{F}$ ]ciprofloxacin to clinical isolates of *E. coli* with MIC values ranging from 0.015  $\mu\text{g/ml}$  to 16  $\mu\text{g/ml}$ . For each MIC value, two strains were studied. The coefficient of correlation ( $R$ ) and the corresponding  $P$  value obtained from linear regression analysis are displayed

**Table 1.** Bacterial binding of [ $^{18}\text{F}$ ]ciprofloxacin (mean  $\pm$  standard deviation,  $n=10$ ) in the absence and presence of unlabelled norfloxacin (first column). [ $^{18}\text{F}$ ]Ciprofloxacin efflux was induced by re-incubation of bacteria with fresh phosphate buffer and [ $^{18}\text{F}$ ]ciprofloxacin remaining in the cell pellet was determined (second column)

	Binding of [ $^{18}\text{F}$ ]ciprofloxacin to <i>E. coli</i> ATCC 25922	
	After one incubation	After efflux
Without norfloxacin	91 $\pm$ 3	12 $\pm$ 1
Plus 100 $\mu\text{g/ml}$ norfloxacin	103 $\pm$ 13	13 $\pm$ 5

treated and untreated *E. coli* cultures. When bacterial cell pellets loaded with [ $^{18}\text{F}$ ]ciprofloxacin were re-incubated at 37°C with fresh phosphate buffer, a rapid efflux of radioactivity was observed (Table 1). On average 13 $\pm$ 1% ( $n=10$ ) of the initially retained radioactivity remained in the pellet after a re-incubation time of 15 min. No further decrease in this value was observed when the re-incubation time was prolonged from 15 min to 30 min. For norfloxacin-pre-treated bacteria, radioactivity efflux was descriptively similar as for untreated cultures (Table 1). When clinical isolates of *E. coli* with different in vitro susceptibility to ciprofloxacin were incubated with [ $^{18}\text{F}$ ]ciprofloxacin (Fig. 2), radiotracer binding appeared to be independent of the respective MIC value ( $R=0.48188$ ;  $P=0.01711$ ).

#### Binding of [ $^{18}\text{F}$ ]ciprofloxacin to blood cells

After incubation of [ $^{18}\text{F}$ ]ciprofloxacin-loaded blood cells with fresh plasma or phosphate buffer, efflux of radioac-

**Table 2.** Microbiological specimens (patients 1–4) isolated from swabs taken from the infected extremity on the study day

Patient	Isolated pathogen	Ciprofloxacin susceptibility
1	<i>Pseudomonas aeruginosa</i>	Moderate
2	<i>Serratia marcescens</i> <i>Staphylococcus epidermis</i>	Yes Not available
3	<i>Serratia marcescens</i> Beta-haemolytic streptococci	Yes Moderate
4	Coagulase-negative staphylococci Corynebacteria	Not available Not available

tivity was observed; 32 $\pm$ 8% ( $n=4$ ) and 21 $\pm$ 6% ( $n=3$ ) of total radioactivity distributed after 10-min incubation time into plasma and phosphate buffer, respectively.

#### PET study in patients

All study procedures were well tolerated by all patients. There was no serious adverse event and no side-effects related to administration of the study medication. Table 2 summarises the microbiological specimens isolated from swabs taken on the study day. Following i.v. injection of [ $^{18}\text{F}$ ]ciprofloxacin into patients, radioactivity cleared rapidly from blood. Figure 3 shows the time-radioactivity profiles measured in whole blood and plasma after i.v. injection of [ $^{18}\text{F}$ ]ciprofloxacin. The terminal elimination half-lives were 201 $\pm$ 35 min and 210 $\pm$ 15 min for the blood and plasma curves, respectively. The profiles of the blood and the plasma curve were almost congruent over the entire observation period. Figure 4 depicts TACs measured with PET in infected and uninfected



tissue of all patients. Peak radioactivity uptake ( $C_{\max}$ ) was descriptively higher in infected as compared to uninfected tissue, with SUV values of  $1.0 \pm 0.2$  and  $0.5 \pm 0.2$ , respectively. Owing to the small sample size, statistical

significance was not reached ( $P=0.068$ , Wilcoxon matched pairs test). The mean times to achieve peak radioactivity uptake ( $T_{\max}$ ) were  $40 \pm 9$  min and  $51 \pm 8$  min for infected and uninfected tissue, respectively. The higher radioactivity uptake in infected tissue resulted in good visualisation of the infected areas on the PET images. Figure 5 shows coronal and transaxial PET images obtained from patient 1. At peak uptake in infected tissue, the ratio between infected and uninfected tissue ranged from 1.8 to 5.5 in individual patients. Following peak uptake, radioactivity was not retained in infected tissue but washed out with similar half-lives as in uninfected tissue. The mean  $T_{1/2}$  values were  $87 \pm 24$  min and  $98 \pm 41$  min for infected and uninfected tissue, respectively.

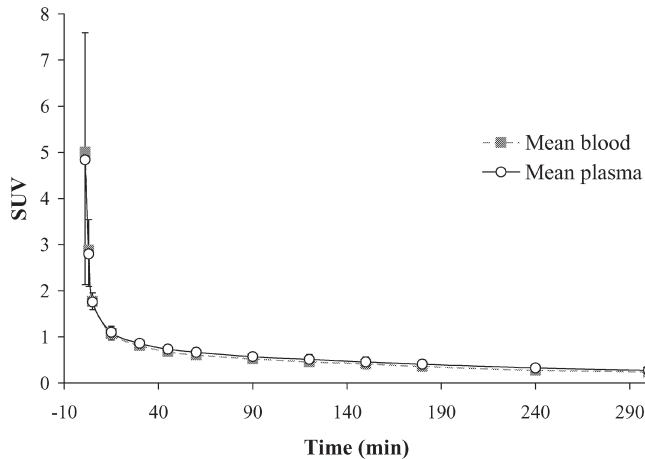


**Fig. 3.** Mean time-radioactivity curve in plasma and whole blood from four patients after intravenous administration of  $725 \pm 9$  MBq [ $^{18}\text{F}$ ]ciprofloxacin. Radioactivity concentration is normalised to the injected radioactivity amount per body weight and expressed as standardised uptake value (SUV)  $\pm$  SD

## Discussion

To the best of our knowledge, no data are available on the binding affinity of ciprofloxacin and the concentration of intracellular bacterial binding sites (i.e. bacterial DNA/DNA gyrase complexes). However, for the structurally related fluoroquinolone norfloxacin, a binding affinity  $K_d$  of about  $1 \mu\text{M}$  to purified DNA/DNA

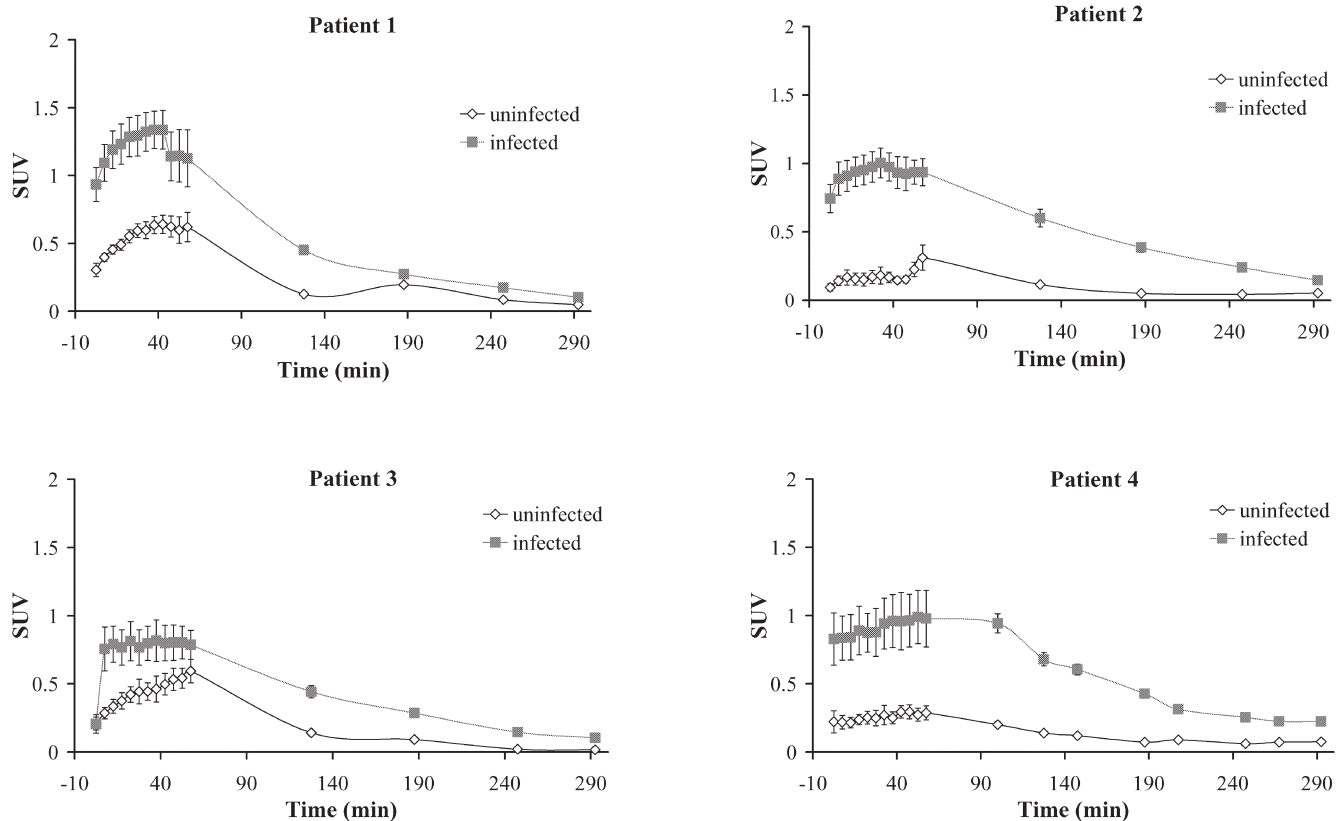


**Fig. 4.** TACs obtained from four patients with microbiologically proven bacterial soft tissue infections of the lower extremities after intravenous administration of [ $^{18}\text{F}$ ]ciprofloxacin ( $725 \pm 9$  MBq). Radioactivity concentrations were measured in the infected limb

and the contralateral uninfected side. Radioactivity concentrations are normalised to the injected radioactivity amount per body weight and expressed as SUV  $\pm$  SD

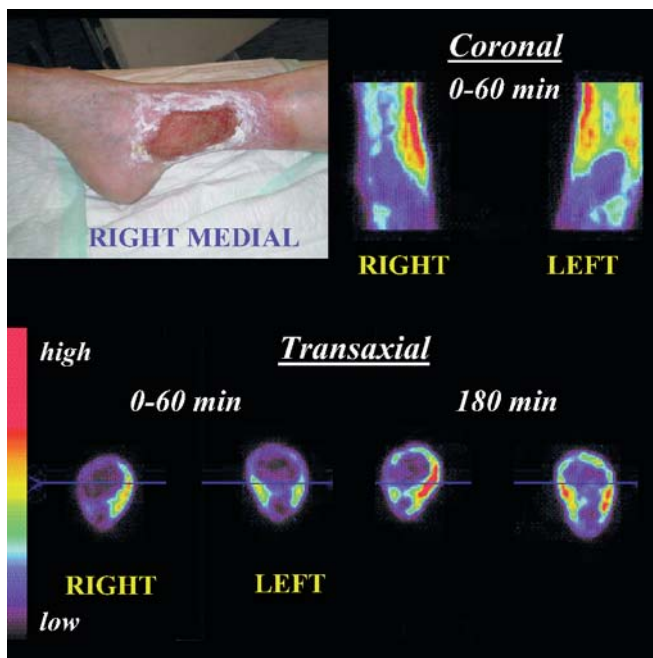


**Fig. 5.** Coronal and transaxial PET images of the lower extremities obtained at 0–60 min and 180 min after i.v. injection of 724 MBq [ $^{18}\text{F}$ ]ciprofloxacin into an 84-year-old woman (patient 1). The patient had microbiologically proven multiple bacterial soft tissue infections on the left and right ankles (*left*: medial and lateral, *right*: medial, see photo)

gyrase complexes has been reported [14]. Such an affinity appears at first sight to be too low for successful visualisation of these binding sites by means of PET. However, several studies have claimed bacteria-specific imaging with a radiolabelled ciprofloxacin analogue, i.e.  $^{99\text{m}}\text{Tc}$ -ciprofloxacin, which is suggested to be irreversibly and specifically trapped inside bacterial cells [3, 15]. It has been proposed that the ability of  $^{99\text{m}}\text{Tc}$ -ciprofloxacin to visualise bacteria is related to the pharmacokinetic and pharmacodynamic properties of ciprofloxacin, which forms part of the radiometallic complex. We therefore assumed that a radiolabelled molecule that is structurally identical to native ciprofloxacin, such as [ $^{18}\text{F}$ ]ciprofloxacin, would display equal or even better specificity for the imaging of bacteria. In addition to bacterial trapping, the known accumulation of ciprofloxacin in white blood cells [16, 17], which migrate to sites of infection, might further contribute to radiotracer retention in infected tissue.

The radiosynthesis of [ $^{18}\text{F}$ ]ciprofloxacin used an isotopic  $^{18}\text{F}$  exchange for  $^{19}\text{F}$  exchange reaction [9] giving a specific radioactivity that was considerably lower than that usually obtained for no-carrier-added  $^{18}\text{F}$ -labelled PET tracers. The average specific radioactivity at the time of injection into patients was  $342 \pm 94$  MBq/ $\mu\text{mol}$ , resulting in the administration of about 0.8 mg unlabelled ciprofloxacin for an injected amount of 725 MBq. This carrier amount is comparable to  $^{99\text{m}}\text{Tc}$ -ciprofloxacin

formulations, which are reported to contain about 2 mg of unlabelled ciprofloxacin [15].

In the first part of this work, we attempted to characterise in vitro the mechanism of binding of [ $^{18}\text{F}$ ]ciprofloxacin to bacterial cells. Interestingly, despite being in clinical use for a relatively long time, no such data have to date been reported for  $^{99\text{m}}\text{Tc}$ -ciprofloxacin. Unfortunately, a direct comparison of our bacterial binding data with  $^{99\text{m}}\text{Tc}$ -ciprofloxacin was not feasible owing to the unavailability of kits for the preparation of this agent. For most in vitro experiments included in the present study, *E. coli* ATCC 25922 was used, since this is a commercially available standardised bacterial strain with good susceptibility against ciprofloxacin (MIC  $< 0.015$   $\mu\text{g}/\text{ml}$ ). We found that binding of [ $^{18}\text{F}$ ]ciprofloxacin to *E. coli* cultures was rapid and non-saturable (Fig. 1). The employed concentrations ranged from concentrations achieved in human tissues after administration of a tracer amount of [ $^{18}\text{F}$ ]ciprofloxacin to those achieved after therapeutic doses of ciprofloxacin [18] (Fig. 1). Addition of an excess of unlabelled norfloxacin to the buffer prior to incubation with [ $^{18}\text{F}$ ]ciprofloxacin failed to reduce bacterial binding compared with untreated bacteria, which further demonstrated the lack of a saturation effect (Table 1). It is important to note that pre-treatment with unlabelled norfloxacin did not result in visible changes of bacterial cells as determined by Gram staining and inspection under a microscope. Bacterial binding of [ $^{18}\text{F}$ ]ciprofloxacin appeared to be readily reversible with rapid efflux of radioactivity after re-incubation of [ $^{18}\text{F}$ ]ciprofloxacin-loaded bacterial cell pellets with fresh phosphate buffer (Table 1). These findings are consistent with a previously published study that found rapid efflux of norfloxacin from *E. coli* cells after incubation with fresh medium [19]. Taken together, our in vitro data do not point to a specific binding process as being responsible for bacterial retention of [ $^{18}\text{F}$ ]ciprofloxacin. It is likely that specific binding to bacterial DNA/DNA gyrase was masked by a high level of non-specific binding.

Bacterial resistance to ciprofloxacin has been discussed as a factor that might limit the applicability of  $^{99\text{m}}\text{Tc}$ -ciprofloxacin for the imaging of bacteria [20]. In order to investigate the relationship between in vitro susceptibility of bacteria and binding of [ $^{18}\text{F}$ ]ciprofloxacin, we incubated clinical isolates of *E. coli* with different MIC values with the radiotracer (Fig. 2). Bacterial binding of [ $^{18}\text{F}$ ]ciprofloxacin appeared to be independent of the respective MIC of the pathogen. The most common mechanism of bacterial resistance to fluoroquinolones is mutation of intracellular binding sites, i.e. bacterial type II topoisomerase enzymes [21]. Since structural alterations of these enzymes as caused by mutations would be expected to decrease specific bacterial binding of [ $^{18}\text{F}$ ]ciprofloxacin, the present findings further corroborate a predominantly non-specific mechanism of retention of the radiolabelled antibiotic in bacterial cells.

In the second part of this work, a PET study was performed in four patients with microbiologically proven bacterial soft tissue infections of the lower extremities. In three patients, at least one of the isolated bacterial species was susceptible to ciprofloxacin (Table 2). In patient 4, susceptibility data were unfortunately not available. Following administration of [ $^{18}\text{F}$ ]ciprofloxacin, sites of infections became rapidly visible on the PET images (Fig. 5). Even at later imaging time points, i.e. 3–4 h after tracer injection, a contrast between infected and uninfected tissue remained. However, when looking at the TACs measured in infected and uninfected tissue of individual patients it appears that radioactivity washes out from infected tissue with a similar  $T_{1/2}$  as for uninfected tissue (Fig. 4), which results in stable or even decreased infected versus non-infected tissue ratios at later imaging time points. Owing to the short physical half-life of  $^{18}\text{F}$  (109.8 min), measurements could not be performed for periods longer than 5 h. Even though some studies with  $^{99\text{m}}\text{Tc}$ -ciprofloxacin have reported that very late imaging time points, i.e. up to 24 h after radiotracer administration [15], are necessary for bacteria-specific imaging with the agent, other studies have reported imaging time points of 4 h, which were also feasible in the present study [3, 22]. The profiles displayed in Fig. 4 are remarkably similar to previously published concentration-time profiles measured with microdialysis in soft tissue infections of patients after therapeutic doses of another fluoroquinolone, i.e. moxifloxacin [23]. In that study, locally increased pharmacokinetic parameters of moxifloxacin (i.e.  $C_{\text{max}}$  and area under the concentration-time curve) were observed in inflamed as compared to uninfected tissue. Even though no attempts were made to measure blood flow in the present study (e.g. with [ $^{15}\text{O}$ ]H $_2$ O), it is likely that the increased uptake of [ $^{18}\text{F}$ ]ciprofloxacin at sites of infection was attributable to increased blood flow and vascular permeability due to local infection. Assuming the presence of a specific binding process, diverging radioactivity versus time profiles between infected and uninfected tissue and an increase in ratios over time would have been expected. The TACs in Fig. 4 display a rapid washout of radioactivity from infected tissue and are thus consistent with non-detectable specific bacterial binding in the *in vitro* experiments.

From the appearance of the TACs shown in Fig. 4 it seems unlikely that local radiotracer binding to components other than bacteria, i.e. leucocytes, exerted an appreciable influence on the kinetics of [ $^{18}\text{F}$ ]ciprofloxacin in infected tissue. However, the congruent time-radioactivity profiles observed in plasma and whole blood (Fig. 3) point to uptake and retention of [ $^{18}\text{F}$ ]ciprofloxacin by cellular components of blood, such as neutrophilic granulocytes and monocytes [16, 17]. When [ $^{18}\text{F}$ ]ciprofloxacin-loaded blood cells were incubated *in vitro* with fresh plasma or phosphate buffer, an efflux of radioactivity was observed, indicating that binding of

[ $^{18}\text{F}$ ]ciprofloxacin to these cells was just as reversible as bacterial binding of the agent. These findings are in accordance with a previous study that found rapid efflux of ciprofloxacin from human neutrophilic granulocytes when the extracellular concentration of the antibiotic was reduced [24].

Taken together, our findings indicate that [ $^{18}\text{F}$ ]ciprofloxacin is not suitable as a bacteria-specific infection imaging tracer. It cannot be excluded that the failure of [ $^{18}\text{F}$ ]ciprofloxacin to visualise bacteria might be related to the low specific radioactivity of the tracer obtained in the exchange labelling method. The reason for the discrepancy between our results and those published with  $^{99\text{m}}\text{Tc}$ -ciprofloxacin is unknown but might be related to different modes of bacterial binding of these two radio-labelled agents.

*Acknowledgements.* The authors wish to thank Bayer AG (Wuppertal, Germany) for supplying unlabelled ciprofloxacin hydrochloride. This study could not have been completed without the excellent technical support of Rainer Bartosch, Gabriele Wagner, Ingrid Leitinger and Bettina Reiterits at the Department of Nuclear Medicine.

## References

1. Corstens FHM, van der Meer JWM. Nuclear medicine's role in infection and inflammation. *Lancet* 1999;354:765–70.
2. Vinjamuri S, Hall AV, Solanki KK, Bomanji J, Siraj Q, O'Shaughnessy E, et al. Comparison of  $^{99\text{m}}\text{Tc}$  infecton imaging with radiolabelled white-cell imaging in the evaluation of bacterial infection. *Lancet* 1996;347:233–5.
3. Hall AV, Solanki KK, Vinjamuri S, Britton KE, Das SS. Evaluation of the efficacy of  $^{99\text{m}}\text{Tc}$ -Infecton, a novel agent for detecting sites of infection. *J Clin Pathol* 1998;51:215–9.
4. Welling MM, Paulusma-Annema A, Balter HS, Pauwels EKJ, Nibbering PH. Technetium-99m labelled antimicrobial peptides discriminate between bacterial infections and sterile inflammations. *Eur J Nucl Med* 2000;27:292–301.
5. Lupetti A, Pauwels EK, Nibbering PH, Welling MM.  $^{99\text{m}}\text{Tc}$ -antimicrobial peptides: promising candidates for infection imaging. *Q J Nucl Med* 2003;47:238–45.
6. Das SS, Hall AV, Wareham DW, Britton KE. Infection imaging with radiopharmaceuticals in the 21st century. *Braz Arch Biol Technol* 2002;45:25–37.
7. Drlica K. Mechanism of fluoroquinolone action. *Curr Opin Microbiol* 1999;2:504–8.
8. Gau W, Kurz J, Petersen U, Ploschke HJ, Wuensche C. Isolation and structural elucidation of urinary metabolites of ciprofloxacin. *Arzneimittelforschung* 1986;36:1545–9.
9. Langer O, Mitterhauser M, Brunner M, Zeitlinger M, Wadsak W, Mayer BX, et al. Synthesis of fluorine-18-labeled ciprofloxacin for PET studies in humans. *Nucl Med Biol* 2003; 30:285–91.
10. Langer O, Mitterhauser M, Wadsak W, Brunner M, Müller U, Kletter K, Müller M. A general method for the fluorine-18 labelling of fluoroquinolone antibiotics. *J Labelled Comp Radiopharm* 2003;46:715–27.

11. Brunner M, Langer O, Dobrozemsky G, Müller U, Zeitlinger M, Mitterhauser M, Wadsak W, Dudczak R, Kletter K, Müller M. [<sup>18</sup>F]Ciprofloxacin, a new PET tracer for non-invasive assessment of ciprofloxacin tissue pharmacokinetics in humans. *Antimicrob Agents Chemother* 2004;48(10):in press.
12. National Committee for Clinical Laboratory Standards. MIC testing. NCCLS 2001; Supplemental tables: M100-S111 (M107).
13. Ricci V, Piddock LJ. Accumulation of norfloxacin by *Bacteroides fragilis*. *Antimicrob Agents Chemother* 2000; 44:2361–6.
14. Shen LL. Molecular mechanisms of DNA gyrase inhibition by quinolone antibacterials. *Adv Pharmacol* 1994;29A:285–304.
15. Britton KE, Wareham DW, Das SS, Solanki KK, Amaral H, Bhatnagar A, et al. Imaging bacterial infection with <sup>99m</sup>Tc-ciprofloxacin (Infecton). *J Clin Pathol* 2002;55:817–23.
16. Bounds SJ, Walters JD, Nakkulka RJ. Fluoroquinolone transport by human monocytes: characterization and comparison to other cells of myeloid lineage. *Antimicrob Agents Chemother* 2000;44:2609–14.
17. Walters JD, Zhang F, Nakkulka RJ. Mechanisms of fluoroquinolone transport by human neutrophils. *Antimicrob Agents Chemother* 1999;43:2710–5.
18. Brunner M, Stass H, Möller JG, Schrolnberger C, Erovcic B, Hollenstein U, Zeitlinger M, Eichler HG, Müller M. Target site concentrations of ciprofloxacin after single intravenous and oral doses. *Antimicrob Agents Chemother* 2002;46:3724–30.
19. Mortimer PGS, Piddock LJV. A comparison of methods used for measuring the accumulation of quinolones by Enterobacteriaceae, *Pseudomonas aeruginosa* and *Staphylococcus aureus*. *J Antimicrob Chemother* 1991;28:639–53.
20. Pauwels EKJ, Welling MM, Lupetti A, Paulusma-Annema A, Nibbering PH, Balter HS. Reply to “Technetium-99m labelled antimicrobial peptides discriminate between bacterial infections and sterile inflammations [letter to the editor]”. *Eur J Nucl Med* 2000;27:1866–8.
21. Hooper DC. Mechanisms of action and resistance of older and newer fluoroquinolones. *Clin Infect Dis* 2000;31(Suppl 2): S24–8.
22. Britton KE, Vinjamuri S, Hall AV, Solanki K, Siraj QH, Bomanji J, Das S. Clinical evaluation of technetium-99m infecton for the localisation of bacterial infection. *Eur J Nucl Med* 1997;24:553–6.
23. Joukhadar C, Stass H, Müller-Zellenberg U, Lackner E, Kovar F, Minar E, Müller M. Penetration of moxifloxacin into healthy and inflamed subcutaneous adipose tissues in humans. *Antimicrob Agents Chemother* 2003;47:3099–103.
24. Easmon CSF, Crane JP. Uptake of ciprofloxacin by human neutrophils. *J Antimicrob Chemother* 1985;16:67–73.